Blunted Refeeding Response and Increased Locomotor Activity in Mice Lacking FoxO1 in Synapsin-*Cre*–Expressing Neurons

Hongxia Ren,[1,2] Leona Plum-Morschel,[1,2] Roger Gutierrez-Juarez,[3] Taylor Y. Lu,[1,2] Ja Young Kim-Muller,[1,2] Garrett Heinrich,[1,2] Sharon L. Wardlaw,[1,2] Rae Silver,[4] and Domenico Accili[1,2]

Successful development of antiobesity agents requires detailed knowledge of neural pathways controlling body weight, eating behavior, and peripheral metabolism. Genetic ablation of FoxO1 in selected hypothalamic neurons decreases food intake, increases energy expenditure, and improves glucose homeostasis, highlighting the role of this gene in insulin and leptin signaling. However, little is known about potential effects of FoxO1 in other neurons. To address this question, we executed a broad-based neuronal ablation of FoxO1 using *Synapsin* promoter–driven Cre to delete floxed *Foxo1* alleles. Lineage-tracing experiments showed that NPY/AgRP and POMC neurons were minimally affected by the knockout. Nonetheless, *Syn-Cre-Foxo1* knockouts demonstrated a catabolic energy homeostatic phenotype with a blunted refeeding response, increased sensitivity to leptin and amino acid signaling, and increased locomotor activity, likely attributable to increased melanocortinergic tone. We confirmed these data in mice lacking the three *Foxo* genes. The effects on locomotor activity could be reversed by direct delivery of constitutively active FoxO1 to the mediobasal hypothalamus, but not to the suprachiasmatic nucleus. The data reveal that the integrative function of FoxO1 extends beyond the arcuate nucleus, suggesting that central nervous system inhibition of FoxO1 function can be leveraged to promote hormone sensitivity and prevent a positive energy balance. ***Diabetes*** **62:3373–3383, 2013**

The alarming increase in the prevalence of obesity and the advances in the ability to genetically map and modify biochemical pathways of hormone action and nutrient sensing have rekindled interest in understanding how the central nervous system (CNS) regulates energy homeostasis and metabolism (1). CNS integration of feeding behavior and nutrient turnover reveals a complex anatomic and functional architecture, with redundant control mechanisms and shared functions that have thus far thwarted attempts at identifying specific networks that can be pharmacologically engaged to control body weight.

Key to solving the stalemate is refinement of our knowledge of the integrated circuitry of CNS metabolic functions. For example, leptin—the main appetite-suppressing hormone—acts at multiple CNS sites in qualitatively different fashions, affecting not only neurohormonal aspects but also reward aspects of feeding (2). Likewise, characterization of specific neuronal populations in areas traditionally linked to food intake, such as the mediobasal hypothalamus (MBH), has revealed a complex pattern of neuronal populations regulating this process as well as interdependent signaling pathways that regulate the activity of these neurons (3,4).

FoxO1 has emerged during the past decade as a critical node in relaying the hormonal status and nutritional status of the organism, allowing target cells to implement transcriptional programs that reflect energy conservation or dispersal. Among its protean functions are the regulation of hepatic glucose production (5,6) and bile acid synthesis (7), the integration of different aspects of pancreatic endocrine function (8), and developmental functions in the differentiation of adipose, muscle, and enteroendocrine progenitor cells (9–11). In the CNS, we and others (12–16) previously have shown that FoxO1 lies astride of insulin and leptin signaling in neuropeptide-producing cells of the arcuate nucleus, orchestrating a complex transcriptional program that includes melanocortin signaling (17) and orphan G-protein-coupled receptors, and whose ultimate outcome is to promote food intake and reduce energy expenditure (18).

The purpose of the current study was to extend our knowledge of the actions of neural FoxO1 beyond the narrow confines of the arcuate nucleus. Impetus for these experiments was provided by the realization that therapeutic modalities based on FoxO1 loss-of-function may be desirable for weight-control purposes. However, to implement such approaches, one needs to map the gamut of pathophysiologic FoxO1 actions in the CNS as a way to ascertain potential liabilities. The studies described in this article were designed to fill this gap.

RESEARCH DESIGN AND METHODS

Experimental animals. The Columbia University Animal Care and Utilization Committee approved all procedures. Normal chow diet included 62.1% of calories from carbohydrates, 24.6% of calories from protein, and 13.2% of calories from fat (PicoLab rodent diet 20, 5053; Purina Mills); high-fat diet (HFD) included 20% of calories from carbohydrates, 20% of calories from protein, and 60% of calories from fat (D12492; Research Diets). We measured weight and length to calculate BMI, and we estimated body composition by nuclear magnetic resonance (Bruker Optics). We generated *Syn*-specific *FoxO* single or triple knockouts by mating *Syn-Cre* transgenic mice with *Foxo1*$^{flox/flox}$ mice or *Foxo1*$^{flox/flox}$*3a* $^{flox/flox}$*4*$^{flox/flox}$ mice (19) and genotyped them as previously described (18). We excluded from analyses knockout mice that showed widespread recombination because of stochastic embryonic expression of *Syn-Cre*. We used cohorts of adult male mice, with 6–8 mice per genotype in most experiments (unless otherwise noted). We used the Rosa-Gfp reporter mice (B6;129-*Gt(ROSA)26Sor*^{tm2sho}/J; JAX Stock Number 004077) for lineage-tracing experiments.

From the [1]Berrie Diabetes Center, New York, New York; the [2]Department of Medicine, Columbia University, New York, New York; the [3]Diabetes Research and Training Center, Albert Einstein College of Medicine, Bronx, New York; and the [4]Department of Psychology, Columbia University, New York, New York.
Corresponding author: Domenico Accili, da230@columbia.edu.
Received 15 April 2013 and accepted 20 June 2013.
DOI: 10.2337/db13-0597
H.R. and L.P.-M. contributed equally to this work.
© 2013 by the American Diabetes Association. Readers may use this article as long as the work is properly cited, the use is educational and not for profit, and the work is not altered. See http://creativecommons.org/licenses/by-nc-nd/3.0/ for details.

Metabolic analyses. We measured food intake with feeding racks (Firma Wenzel). For refeeding experiments, we habituated mice to feeding racks for 3 days, fasted them for 18 h, placed feeding racks 2 h after the start of the light phase, and measured food intake thereafter. We used a TSE Labmaster Platform (TSE Systems) for indirect calorimetry and activity measurements (17). For mice receiving adenovirus injection, we measured the wheel-running activity after the established protocol (20). Briefly, wheel-running activity was monitored remotely by Vitalview (Minimitter, Bend, OR), with counts collected in 10-min bins, and visualized using double-plotted actograms. We measured blood glucose by the One-Touch Ultra meter (LifeScan, Milpitas, CA), insulin and leptin were measured by ELISA, glucagon was measured by radioimmunoassay (Linco Research, St. Charles, MO), plasma free fatty acids and cholesterol were measured by nonesterified fatty acid hazard ratio and cholesterol-E test reagents, respectively (Wako Chemicals, Richmond, VA), and triglycerides were measured by serum triglyceride determination kit (Sigma-Aldrich, St. Louis, MO). Body composition was determined using Bruker Minispec nuclear magnetic resonance (Bruker Optics, Billerica, MA). We performed euglycemic-hyperinsulinemic clamps as previously described (21).

Immunostaining. We perfused mice with saline and then with 4% paraformaldehyde. We froze brains in Tissue-Tek O.C.T. Compound (Sakura) and cut 30-μm–thick coronal sections for green fluorescent protein (GFP)-specific immunohistochemistry (Molecular Probes/Invitrogen). We acquired images with a Nikon eclipse microscope.

RNA procedures. We extracted RNA with Trizol (Invitrogen) and performed quantitative PCR using SYBR Green I (Roche). Primer sequences are available on request. We used equal amounts of total RNA for reverse transcription and measured threshold cycle for each gene. β-Actin was used as an internal control. Data were quantified by standard delta ratio threshold cycle method.

Hypothalamic neuropeptide assays. We extracted MBH in 0.1 N HCl. We measured β-endorphin and α-melanocyte–stimulating hormone (MSH) by radioimmunoassay (17).

Statistical analyses. We analyzed data with Student *t* test, one-way ANOVA, or two-way ANOVA. $P < 0.05$ was considered statistically significant ($^*P < 0.05$; $^{**}P < 0.01$; $^{***}P < 0.001$).

RESULTS

Generation and analysis of neuronal FoxO1 knockout mice. To generate neuron-specific FoxO1 knockout mice, we crossed *Foxo1*$^{lox/lox}$ and *Syn-Cre* mice. Cre-mediated deletion of the lox*P*-flanked *Foxo1* exon 2 resulted in null *Foxo1* alleles in Synapsin-expressing neurons (hereafter called *Syn-Foxo1*). To assess the distribution of *Foxo1* ablation in the CNS, we introduced a reporter allele that encodes GFP as a marker of Cre-mediated recombination. GFP immunohistochemistry revealed Cre-mediated recombination across the brain, including cortex, hippocampus, and multiple hypothalamic nuclei. The frequency of *Syn-Cre*–mediated recombination varied in different brain regions. Hippocampus and dorsal medial nucleus showed the highest fractions of recombined cells, whereas cortex, ventral medial nucleus, and paraventricular hypothalamic nucleus had fewer GFP$^+$ cells. The arcuate nucleus showed limited recombination, and the suprachiasmatic nucleus (SCN) showed little if any recombination (Fig. 1*A*). To provide a quantitative assessment of *Foxo1* deletion, we assayed recombination using genomic DNA extracted from various brain regions. These data are consistent with the immunohistochemistry and also show extensive recombination in the brain stem, but not in peripheral tissues (Fig. 1*B*).

Limited *Syn-Cre*–mediated recombination in NPY/AgRP and POMC neurons. FoxO1 ablation in MBH AgRP/NPY and POMC neurons has striking effects on energy homeostasis and peripheral metabolism (17,18). To assess potential contributions of FoxO1 ablation in these neurons to the overall phenotype of *Syn-Foxo1* mice, we determined the extent of *Syn-Cre*–mediated recombination in these two neuronal populations. To this end, we generated double-transgenic mice in which neurons undergoing *Syn-Cre*–mediated recombination was labeled red by a *Rosa-Tomato* allele (*Syn-Tom*) (22), whereas NPY/AgRP or POMC neurons were labeled green by *Npy-Gfp* or *Pomc-Gfp* transgenes, i.e., *Syn-Tom;Npy-Gfp* (Fig. 2*A–E*) and *Syn-Tom;Pomc-Gfp* (Fig. 2*F–J*), respectively. Double fluorescence demonstrated that *Npy*-labeled or *Pomc-Gpf*–labeled neurons had minimal overlap with *Syn-Tom* neurons (Fig. 2*A*, *B*, *F*, and *G*). We quantified the

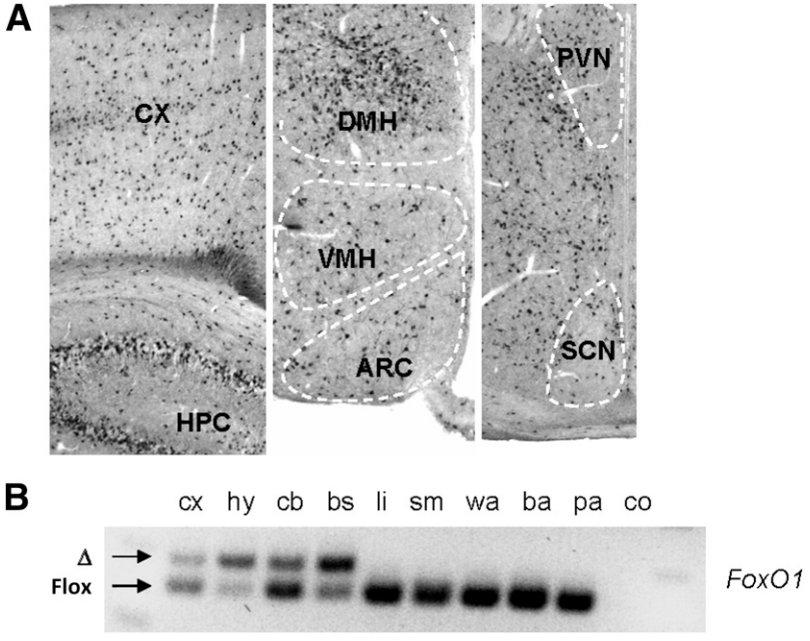

FIG. 1. Generation of *Syn-Foxo1*$^{-/-}$ mice. *A*: GFP immunohistochemistry in the hypothalamus of *Syn-Gfp* mice as a reporter of Cre-mediated recombination (black) in cortex (CX), hippocampus (HPC), and various hypothalamic nuclei (dorsal medial nucleus [DMH], ventral medial nucleus [VMH], arcuate nucleus [ARC], paraventricular hypothalamic nucleus [PVN], and SCN). *B*: Detection of recombined *Foxo1* allele in brain, including cortex (cx), hypothalamus (hy), cerebellum (cb), and brain stem (bs), but not in other tissues, including liver (li), skeletal muscle (sm), white adipose tissue (wa), brown adipose tissue (ba), and pancreas (pa), or in wild-type control (co).

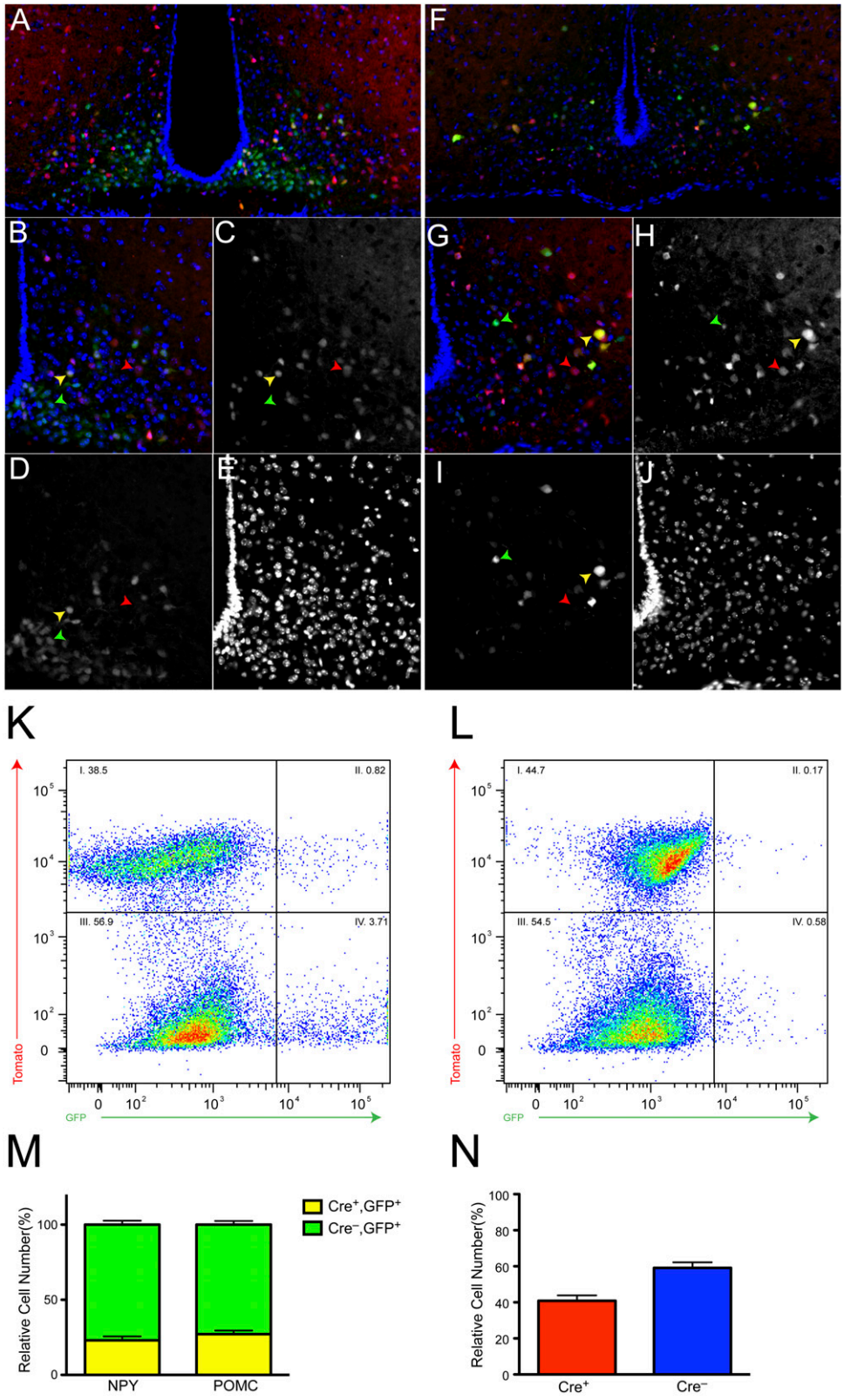

FIG. 2. Limited *Syn-Cre*–mediated recombination in NPY-AgRP and POMC neurons. *A–J*: Fluorescence microscopy of arcuate nucleus from *Syn-Cre;Rosa-Tomato* mice carrying *Npy-Gfp* (*A–E*) or *Pomc-Gfp* (*F–J*) transgene. Neurons exhibiting *Syn-Cre*–mediated recombination are labeled red and those expressing *Npy-Gfp* (*A*) or *Pomc-Gfp* (*F*) are green. Double-positive neurons are yellow. Magnified merged views (*B*, *G*) showing limited overlapping and individual channels for *Tomato* (*C*, *H*), *Npy-Gfp* (*D*), *Pomc-Gfp* (*I*), and DAPI (*E*, *J*). *K* and *L*: Representative fluorescence-activated cell sorting analysis of dissociated hypothalamic neurons of *Syn-Cre;Rosa-Tomato;Npy-Gfp* mice (*B*) and *Syn-Cre;Rosa-Tomato;Pomc-Gfp* mice (*C*). The percentage of each quadrant over the total sorted cells is listed. *M*: Quantification of the percentage of NPY or POMC neurons with active *Syn-Cre* by fluorescence-activated cell sorting analysis ($n = 3$). *N*: Quantification of the percentage of *Syn-Cre*–recombined neurons in the hypothalamus by fluorescence-activated cell sorting analysis ($n = 6$).

findings using fluorescence-activated cell sorting in which double-labeled neurons were distinct from single-labeled neurons (Fig. 2*K* and *L*, *upper* and *lower right quadrants*, respectively). *Syn-Tom* neurons accounted for ~20% of NPY neurons, ~20% of POMC neurons (Fig. 2*M*), and ~40% of hypothalamic neurons (Fig. 2*N*). We estimated that NPY and POMC neurons combined constitute <5% of total sorted MBH neurons. Thus, we conclude that *Syn-Cre* primarily targets neurons other than NPY and POMC in the hypothalamus.

Increased central hormonal and nutrient sensitivity in *Syn-Foxo1* mice. We evaluated *Syn-Foxo1* mice by measuring plasma metabolites and energy expenditure with different diets. In chow-fed animals, we did not detect differences in body weight and composition, or in plasma triglycerides (Table 1). Measurements of respiratory exchanges failed to reveal alterations of V_{O_2} and V_{CO_2}, indicating that basal energy homeostasis was unaltered (data not shown).

However, when we measured the response to fasting and refeeding, we found that *Syn-Foxo1* mice fed significantly less after an overnight fast (Fig. 3*A*). Specifically, during the 6-h refeeding, wild-type and knockout mice consumed 0.3831 and 0.2921 kcal/g body weight (calories normalized by body weight), respectively. To explain this observation, we measured hormonal sensitivity. Serum leptin levels were significantly decreased in fasted and ad libitum–fed *Syn-Foxo1* mice (Fig. 3*B*). We examined leptin signaling by immunohistochemistry with antiphospho-Stat3 (pStat3) antibody in refed mice. The number of cells displaying pStat3 immunoreactivity and the intensity of the signal increased nearly two-fold in *Syn-Foxo1* mice (Fig. 3*C*). Next, we examined whether the increase in leptin signaling was cell-autonomous. To this end, we generated *Syn-Foxo1* mice bearing a *Rosa-Tom* allele and measured pStat3 immunoreactivity in response to refeeding after an overnight fast. The expectation of this experiment was that if the decreased rebound food intake was attributable to increased leptin sensitivity in FoxO1-deficient neurons, then knockout mice should show increased pStat3 signal (green fluorescence) in neurons that were marked by FoxO1 ablation (red fluorescence), giving rise to yellow fluorescence. We observed that most of the pStat3 signal colocalized with recombined neurons, indicating that FoxO1 ablation increases leptin-induced pStat3 generation in a cell-autonomous manner (Fig. 3*D*).

Hypothalamic amino acid signaling regulates satiety and feeding behaviors (23). We measured amino acid sensitivity by immunostaining with antibody to the mTOR substrate, phospho-ribosomal protein S6 (pS6). *Syn-Foxo1* mice had increased pS6, predominantly in dorsal medial nucleus (Fig. 3*E*), a site of *Syn-Cre*–dependent recombination (Fig. 1*A*). Using *Syn-Tom* to label recombined neurons, we sought to determine whether the increase of pS6 was caused by FoxO1 deletion in a cell-autonomous or cell-nonautonomous manner. We saw that increased pS6 staining occurred equally in FoxO1-deleted and FoxO1-intact dorsal medial nucleus neurons, indicating that the effect of FoxO1 ablation is at least partly cell-nonautonomous (Fig. 3*F*).

Altered insulin secretion in *Syn-Foxo1* mice. The CNS further regulates pancreatic hormone secretion, especially through the adrenosympathetic system (24). We therefore measured insulin secretion induced by the β3-adrenergic receptor agonist, CL-316243. Activating β3-adrenergic receptor quickly increases insulin secretion by pancreatic β-cells and free fatty acid release by adipocytes. After CL-316243 injection, *Syn-Foxo1* mice showed consistently lower glucose (Fig. 4*A*), secondary to increased insulin release (Fig. 4*B*). Serum free fatty acid levels were comparable with those of controls (Fig. 4*C*), indicating that the effect of the *Foxo1* mutation on insulin release is not secondary to increased lipolysis with β3-adrenergic receptor agonist stimulation. Next, we examined insulin secretion in static incubations of purified pancreatic islets and found small but significant increases induced by low (5 mmol/L) and high (25 mmol/L) glucose concentrations (Fig. 4*D*). Total insulin content and secretion in response to KCl-induced depolarization were comparable (Fig. 4*D*). Islet size tended to be larger in *Syn-Foxo1* animals, but not significantly larger (Fig. 4*E*). These data indicate that FoxO1 ablation in *Syn-Cre* neurons increased sympathoadrenal responses. Using the *Syn-Tom* reporter, we found no evidence of Cre-mediated recombination in the pancreas of *Syn-Foxo1* animals (data not shown), effectively ruling out a direct effect of FoxO1 ablation in β-cells (25). The increased insulin secretion from β-cells in response to adrenosympathetic stimuli did not alter fasted and fed glucagon levels (Fig. 4*F*). However, *Syn-Foxo1* mice exhibited significantly lower circulating insulin levels (Table 1), indicating increased insulin sensitivity.

TABLE 1
Metabolic measurements

		WT	*Syn-Foxo1*	*P*
Weight, g		28.64 ± 1.27	27.77 ± 0.77	NS
Body composition, %	Fat mass	12.9 ± 2.5	14.3 ± 1.1	NS
	Lean mass	73.2 ± 1.5	73 ± 1	NS
Glucose, mg/dL	Ad libitum	136 ± 10	124 ± 3	NS
	Fasted	66 ± 3	66 ± 4	NS
	Refed	174 ± 14	159 ± 5	NS
	Fasted (HFD)	87 ± 7	68 ± 4	<0.05
Insulin, ng/mL	Ad libitum	3.3 ± 0.4	1.8 ± 0.4	<0.03
	Fasted	0.6 ± 0.1	0.5 ± 0.1	NS
	Refed	7.7 ± 1.1	4.7 ± 0.7	<0.05
Triglyceride, mg/dL	Ad libitum	117 ± 20	165 ± 14	NS

Fasting measurements were performed after an overnight fast. Refed measurements were performed 4–6 h after refeeding. Ad libitum samples were collected 2–3 h after lights-on for 13- to 16-week-old male knockout mice and control littermates fed chow diet unless otherwise indicated. Data are means ± SEM. N = 8–10 for each genotype and measurement. WT, wild-type; NS, not significant.

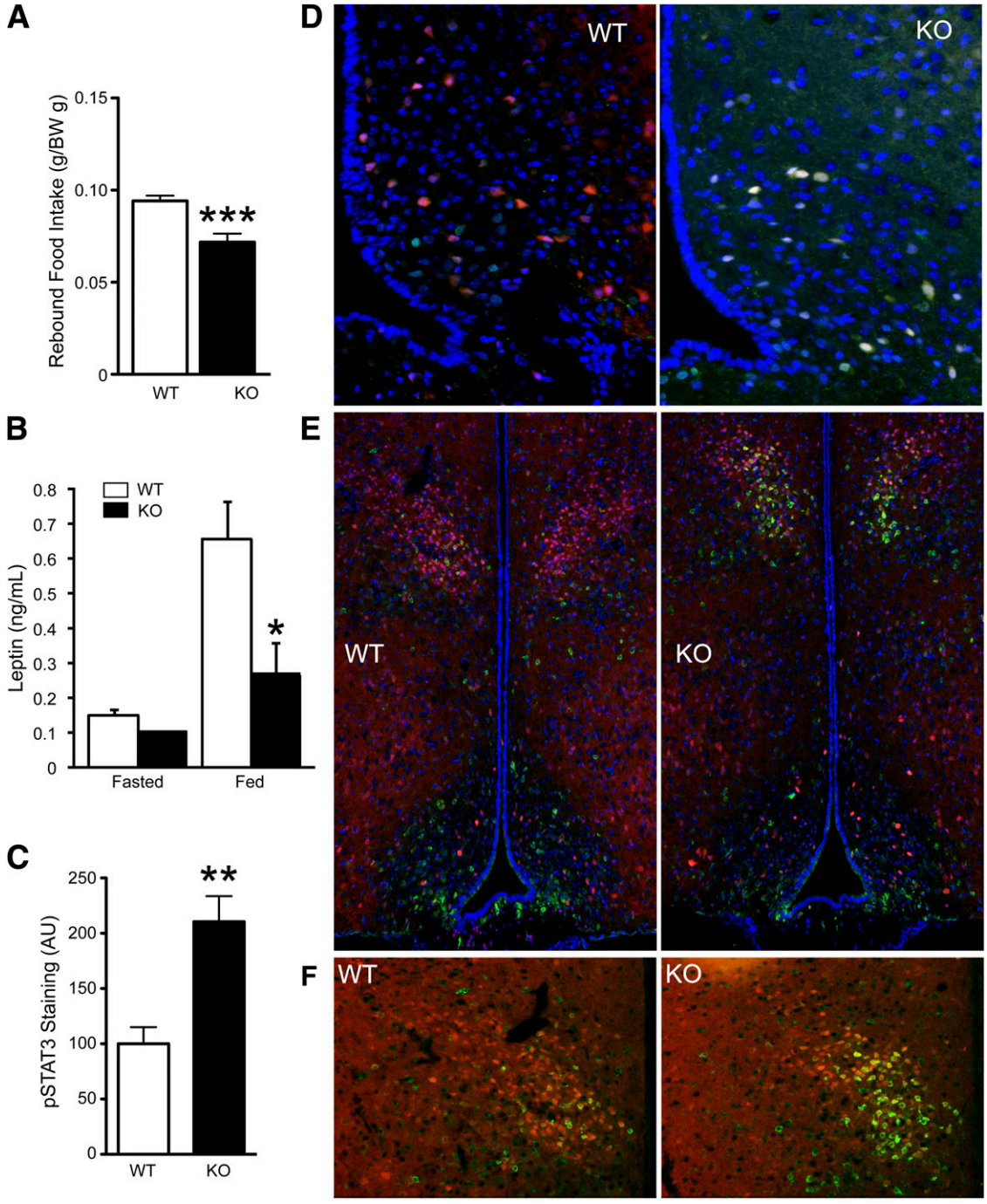

FIG. 3. Increased central hormonal and nutrient sensitivity in *Syn-Foxo1* mice. *A*: Rebound food intake after an overnight fast (n = 6 for each genotype). *B*: Serum leptin measured after overnight fasting or refeeding (n = 6–8 for each genotype). *C*: Quantification of the integrated intensity of pSTAT3 staining in the arcuate nucleus from refed wild-type and *Syn-Foxo1*$^{-/-}$ mice (n = 6). *D*: pStat3 staining (green) in the arcuate nucleus from refed wild-type (*Syn-Foxo1*$^{+/+}$*;Rosa-Tomato*) and knockout (*Syn-Foxo1*$^{-/-}$*;Rosa-Tomato*) mice. *Syn-Cre* neurons are labeled in red. Nuclei are staining with DAPI (blue). *E*: Increased pS6 staining (green) in the hypothalamus from *Syn-Foxo1;Rosa-Tomato* mice. *Syn-Cre*–recombined neurons are labeled in red. Nuclei are staining with DAPI (blue). *F*: pS6 staining (green) in dorsal medial nucleus of the hypothalamus from *Syn-Foxo1;Rosa-Tomato* and control mice. AU, arbitrary units; BW, body weight; KO, knockout; WT, wild-type. *P < 0.05; **P < 0.01; ***P < 0.001.

Increased locomotor activity and melanocortin signaling in *Syn-Foxo1* mice. Male *Syn-Foxo1* mice had increased locomotor activity during the dark phase of the light cycle (Fig. 5*A*). Previous studies have shown that FoxO1 ablation in POMC neurons increased locomotor activity because of increased α-MSH processing and melanocortin signaling (17). Given that only a minority of POMC neurons were targeted in *Syn-Foxo1* mice (Fig. 2), the cause of increased locomotion in *Syn-Foxo1* mice is likely different from that for *Pomc-Foxo1* knockout mice. In fact, α-MSH and β-endorphin levels in the MBH were comparable between wild-type and *Syn-Foxo1* mice (Fig. 5*B* and *C*), indicating that processing of POMC-derived hormones occurs normally in the knockout mice. The α-MSH is rapidly metabolized in vivo by prolyl-carboxypeptidase (Prcp) (26). The ratio of α-MSH to β-endorphins in *Syn-Foxo1*

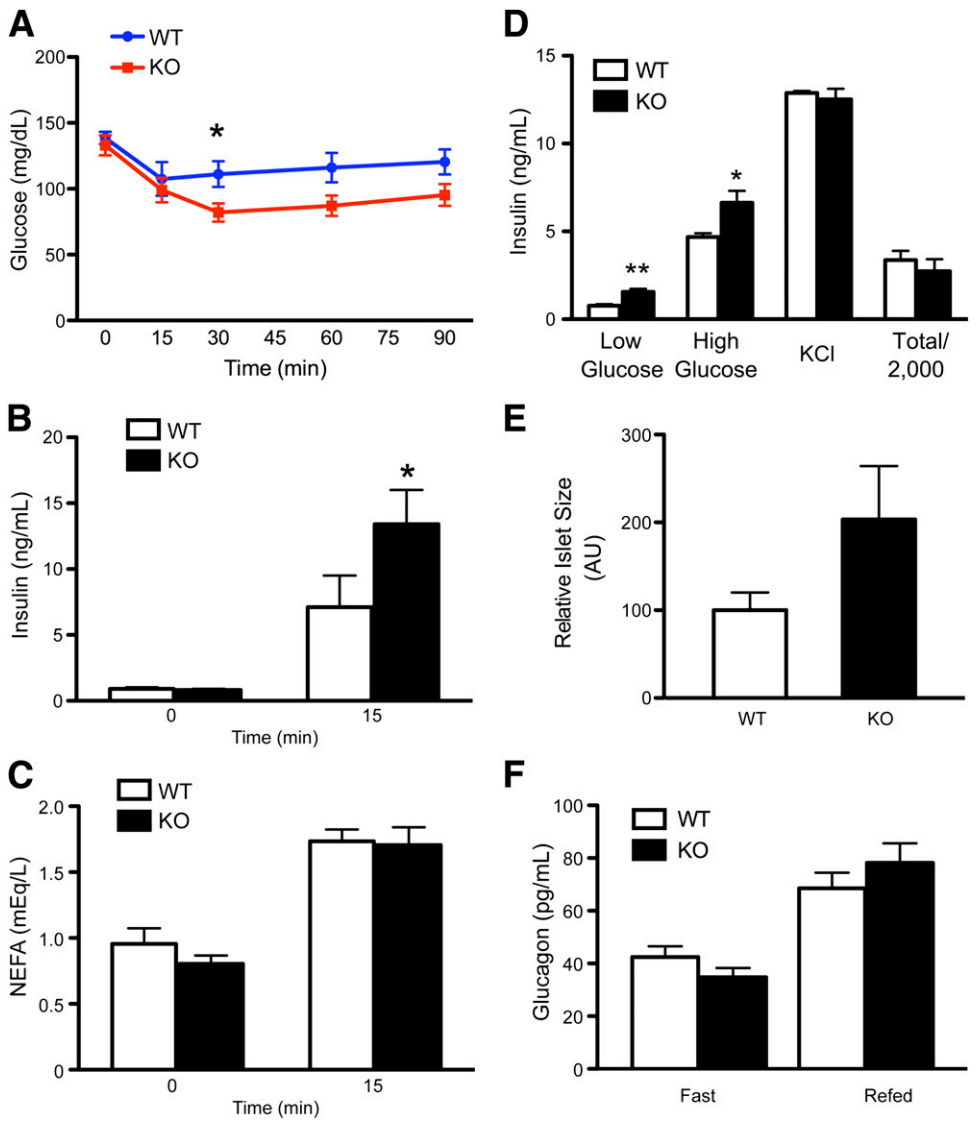

FIG. 4. Altered brain–pancreas axis in *Syn-Foxo1*$^{-/-}$ mice. Glucose (*A*), insulin (*B*), and nonesterified fatty acid (*C*) levels after β3-adrenergic receptor agonist injection (n = 7 for each genotype). *D*: Insulin secretion from islets isolated from *Syn-Foxo1* and wild-type mice (n = 8 for each genotype). Total/2,000: 1:2,000 dilution of islet insulin content obtained by acid extraction. *E*: Islet size quantification by morphometry (n = 6–8 for each genotype). *F*: Fasted and fed glucagon levels (n = 6–8 for each genotype). AU, arbitrary units; KO, knockout; NEFA, nonesterified fatty acid; WT, wild-type. *$P < 0.05$; **$P < 0.01$.

mice was slightly higher compared with that of wild-type mice (0.471 ± 0.025 vs. 0.419 ± 0.014, respectively; P = not significant), consistent with the possibility that slower inactivation of α-MSH may contribute to increased melanocortinergic tone. α-MSH signaling exerts negative feedback regulation on its peptide processing, reducing Pcsk1 expression (17). *Pcsk1* and *Prcp* expression were significantly reduced in the hypothalamus of *Syn-Foxo1* mice during the phase of increased locomotor activity (Fig. 5*E* and *F*). These data suggest that increased melanocortin signaling in *Foxo1* knockout mice contributes to the increased locomotor activity.

We tested this hypothesis by a gain-of-function approach. We reasoned that if FoxO1 loss-of-function increased locomotor activity, then a gain-of-function mutant should reverse this phenotype. We injected adenovirus encoding the constitutively active FoxO1-ADA mutant (9) into the MBH. After this manipulation, we observed increased hypothalamic *Foxo1* when compared with mice that received control GFP adenovirus (Fig. 5*G*). After recovery, we individually housed mice in activity hotels provided with a running wheel and monitored wheel rotations to assess locomotor activity during the 24-h light–dark cycle. Mice injected with FoxO1-ADA showed less locomotor activity during the dark phase (Fig. 5*H*). Of note, as a negative control, mice with FoxO1-ADA injection into the SCN—a site spared by *Syn-Cre* recombination—demonstrated no change in activity patterns (data not shown). The SCN is the site of the master clock of the brain, and it known for its role in controlling daily rest–activity rhythms. This result indicates that the activity phenotype is not caused by changes in SCN.

Single and triple FoxO ablation in neurons protect equally from HFD-induced weight gain. We next investigated whether the comparatively mild phenotype seen in *Syn-Foxo1* mice could be explained by compensatory actions of the two closely related isoforms, FoxO3 and FoxO4 (19). To this end, we generated triple-knockout

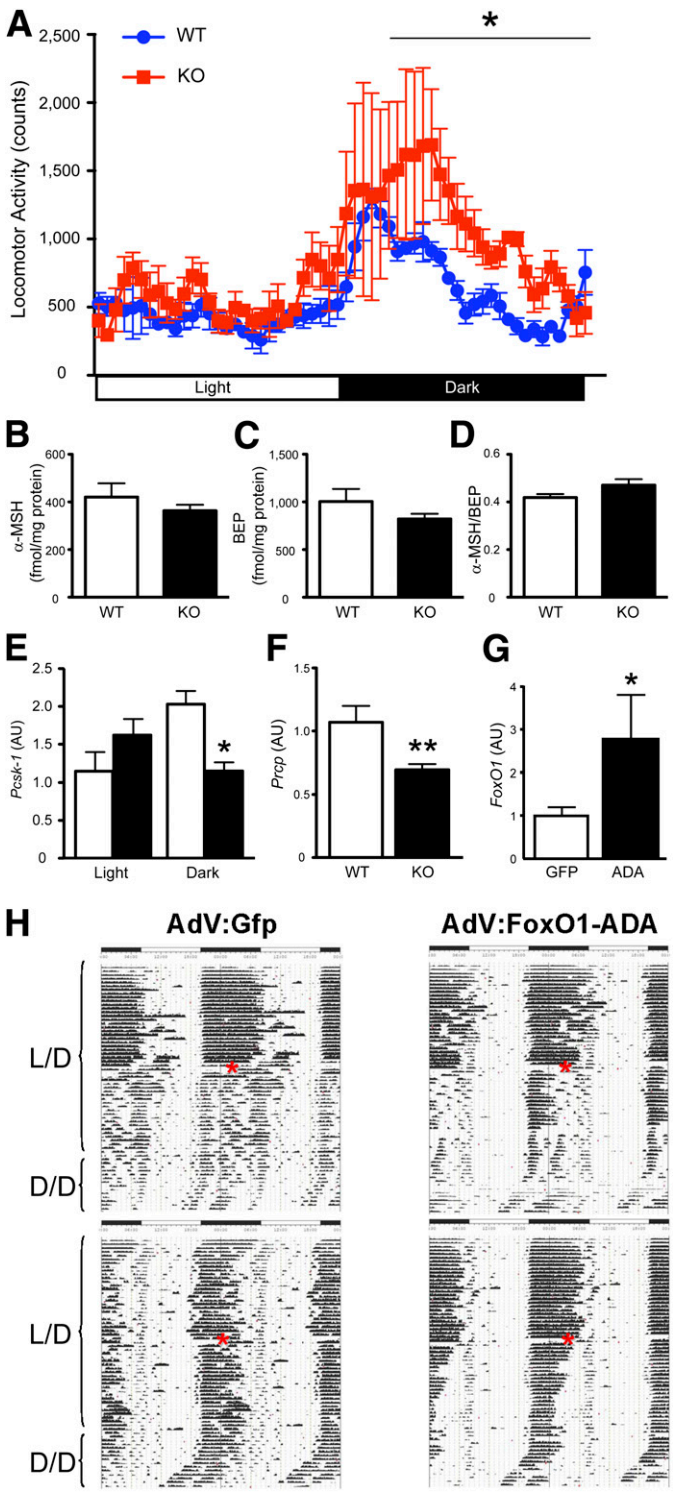

FIG. 5. Locomotor activity and melanocortin signaling in single and triple *Syn-Foxo* knockout mice. *A*: Locomotor activity during the 24-h light-dark cycle in *Syn-Foxo1,3,4* and control wild-type mice (n = 8 for each genotype). We measured activity by beam breaks in metabolic chambers used for indirect calorimetry studies. The α-MSH (*B*), β-endorphin (*C*), and α-MSH:BEP ratios (*D*) in *Syn-Foxo1* and control wild-type mice (n = 8–9 for each genotype) are shown. *Pcsk1* (*E*) and *Prcp* (*F*) mRNA levels during the dark phase of the light cycle (n = 6–8 for each genotype). *G*: *Foxo1* mRNA in the MBH after delivery of FoxO1-ADA or GFP adenovirus (n = 6 for each genotype). Data are expressed as fold-change compared with control (normalized to 1). *H*: Locomotor activity after delivery of FoxO1-ADA or GFP adenovirus. Activity was measured by wheel rotations for each individually housed mouse with a running wheel during 12-h light/12-h dark cycle or continuous 24-h dark cycle. We show two representative continuous activity recordings over 48 h for each genotype. Red asterisk depicts the time of viral injection. AU, arbitrary units; BEP, β-endorphin; D/D, 24-h dark cycle; KO, knockout; L/D, 12-h light/12-h dark cycle; WT, wild-type. *P < 0.05; **P < 0.01.

mice using *Syn-Cre* (*Syn-Foxo1,3,4*). mRNA measurements in hypothalamus and hippocampus from wild-type and *Syn-Foxo1,3,4* mice revealed significant reductions of *Foxo1* and *Foxo3*, whereas *Foxo4* was undetectable (Fig. 6*A*). *Syn-Foxo1,3,4* and wild-type mice showed comparable body weight when fed the normal chow diet (Fig. 6*B*). When fed HFD after weaning, triple-knockout mice gained less weight compared with wild-type mice (Fig. 6*C*), likely because of reduced fat accumulation, as indicated by body composition studies (Fig. 6*D*).

Next, we determined whether the knockout protected from weight gain induced by HFD feeding. We used mice backcrossed onto B6 background to minimize individual variation. Wild-type mice rapidly gained weight when fed HFD, whereas knockout mice consistently maintained a significantly lower body weight (Fig. 6*E*). We analyzed body composition after 4 months of HFD feeding and found that knockout mice had significantly less fat mass compared with wild-type mice (Fig. 6*F*). We compared these mice with triple *Syn-Foxo1,3,4* mice, and we found that the extent of protection from HFD-induced fat accumulation was the same. The triple-knockout mice fed HFD had lower body weight than wild-type mice (33.8 ± 0.8 g; knockout mice: 31.3 ± 0.7 g; P = 0.035). Then, we analyzed energy balance in this cohort by indirect calorimetry. Interestingly, knockout mice had significantly increased V_{O_2} (Fig. 6*G*), locomotor activity, and energy expenditure during both light and dark phases (Fig. 6*H* and *I*). Knockout mice had respiratory quotients comparable with those of wild-type mice (Fig. 6*J*). In conclusion, FoxO1 ablation in *Syn-Cre*–expressing neurons increased energy expenditure in HFD-fed animals and partly offset diet-induced weight gain.

Distinct energy balance and glucose homeostasis phenotypes of *Pomc;Agrp-Foxo1* mice. POMC and AgRP neurons in the arcuate nucleus are critical CNS components for controlling metabolic homeostasis. We have reported that knocking out FoxO1 in either POMC or AgRP neurons improves energy and glucose homeostasis (17,18). Curiously, we found that only few POMC and AgRP neurons undergo *Syn-Cre*–mediated recombination (Fig. 2), yet *Syn-Foxo1* mice have an improved metabolic profile (Fig. 3). To distinguish the collective contribution of POMC and AgRP neurons from that of other CNS neurons, we characterized the phenotype of mice with combined FoxO1 knockout in both POMC and AgRP neurons. In contrast to *Syn-Foxo1* mice, *Pomc;Agrp-Foxo1* mice fed normal chow exhibited a lean phenotype, with lower body weight (Fig. 7*A*), decreased fat mass (Fig. 7*B*), and increased lean mass (Fig. 7*C*). Furthermore, during the 24-h light cycle *Pomc;Agrp-Foxo1* mice showed significantly reduced V_{O_2} (Fig. 7*D*) and elevated respiratory quotient but unaltered locomotor activity (Fig. 7*E*) compared with wild-type mice.

Considering this energy partitioning phenotype, we analyzed hepatic glucose production in *Pomc;Agrp-Foxo1* mice by euglycemic-hyperinsulinemic clamp studies. Glucose infusion rates trended higher in *Pomc;Agrp-Foxo1* mice (Fig. 7*G*), likely because of increased rates of glucose disposal (Fig. 7*H*), but neither difference reached statistical significance. Interestingly, hepatic glucose production

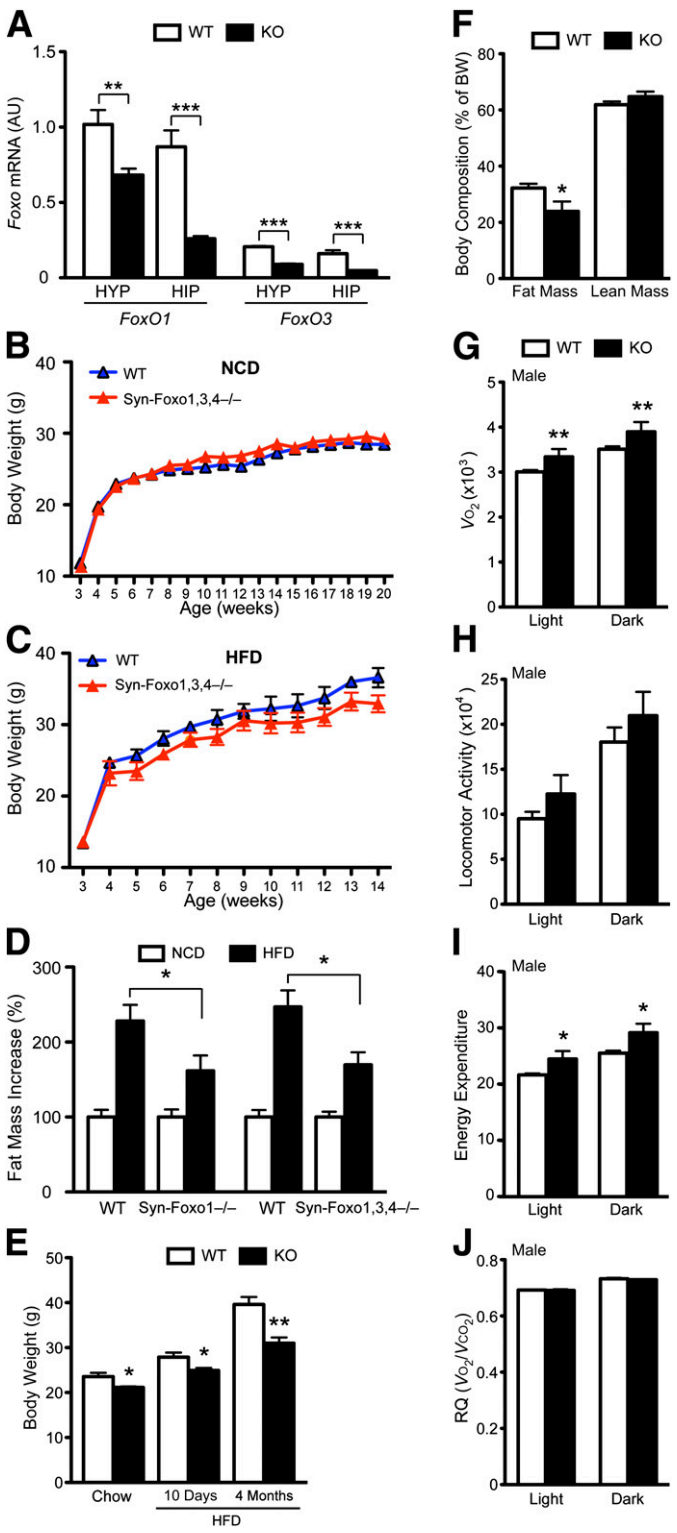

FIG. 6. FoxO ablation in neurons protects from HFD-induced weight gain. *A*: *Foxo* mRNA levels in the hypothalamus and hippocampus (n = 6–8 for each genotype). *B* and *C*: Growth curve of *Syn-Foxo1,3,4* and wild-type mice fed chow (n = 32–35 for each genotype; *B*) or HFD (n = 6 for each genotype; *C*). *D*: Body composition of mice fed HFD (n = 6–10 for each genotype). Body weight (*E*) and body composition (*F*) of *Syn-Foxo1* and wild-type mice fed HFD at 11 weeks of age (n = 5–6 for each genotype). *G–J*: Indirect calorimetry measurements. Oxygen consumption (mL/h/kg) (*G*), locomotor activity (counts) (*H*), energy expenditure (W/kg) (*I*), and respiratory quotient (*J*) of male mice fed HFD (n = 8 for each genotype). AU, arbitrary units; BW, body weight; HIP, hippocampus; HYP, hypothalamus; KO, knockout; NCD, normal chow diet; RQ, respiratory quotients; WT, wild-type. *P < 0.05; **P < 0.01; ***P < 0.001.

was unchanged (Fig. 7*I*), unlike in *Agrp-Foxo1* mice (18). Based on these results, we conclude that FoxO1 function in POMC and AgRP has concordant effects to increase energy expenditure but has opposing actions on hepatic glucose production, as intimated by a previous study (21). The metabolic functions of FoxO1 in *Syn-Cre*–expressing neurons appear to be distinct from those in AgRP and POMC neurons.

DISCUSSION

In this work, we describe the metabolic and energy balance phenotypes associated with deletion of transcription factor FoxO1, a key metabolic sensor, in *Syn-Cre*–expressing neurons that are found scattered in the cortex, hippocampus, hypothalamus, and brain stem. *Syn-Foxo1* mice display a catabolic energy balance phenotype associated with increased sensitivity to hormone and nutrient signaling within the CNS and increased locomotor activity, possibly attributable to low α-MSH turnover leading to enhanced melanocortin signaling. The heterogeneity of *Syn-Cre*–mediated recombination, as assessed by lineage tracing, limits our ability to assign the observed phenotype to a specific neuronal subtype. Nonetheless, we used three alternative approaches to begin to map the functional neuroanatomy of FoxO functions in the CNS. First, lineage-tracing approaches show that only ~20% of NPY/AgRP and POMC neurons display *Syn-Cre*–dependent recombination, effectively ruling a major contribution of these key neuronal populations to the energy balance and metabolic phenotypes of *Syn-Foxo1* mice. We supported this conclusion by analyzing mice with combined ablations of FoxO1 in AgRP and POMC neurons, and by showing that the phenotypes differ. Second, concurrent ablation in *Syn-Cre* neurons of the three insulin-regulated FoxO isoforms, FoxO1, FoxO3, and FoxO4, also conferred a catabolic energy expenditure phenotype, with improved glucose metabolism and resistance to HFD, demonstrating that FoxO functions likely overlap, similar to previous observations (6,27). Third, we used a gain-of-function approach to map the increased activity phenotype to the MBH. We conclude that in addition to their established role in neuropeptide synthesis and processing, FoxO1, FoxO3, and FoxO4 have anabolic functions in other areas of the CNS.

A new finding of the present work is the increase in insulin secretion observed in response to a β3-AR agonist. This likely reflects an effect of FoxO1 on sympathetic activity, possibly because of loss of FoxO1 function in the brain stem (28,29). Our conclusion is that the integrative neuronal function of FoxO1 extends beyond the arcuate nucleus, suggesting that broad-based inhibition of FoxO1 function in the CNS can promote hormone sensitivity and prevent metabolic disease.

Key components of insulin and leptin signaling pathways have been studied using pan-neuronal ablation approaches (30). Our data emphasize that there is no such thing as a truly pan-neuronal knockout, and that caution should be exerted in comparing knockouts performed with different Cre drivers. Mice with *Nestin-Cre*–driven insulin receptor knockout (31) develop diet-induced obesity with increases in body fat, mild insulin resistance, increased plasma leptin, and hypertriglyceridemia, demonstrating that neuronal insulin receptor function affects energy balance. With the caveats stated, it is reassuring that the overall direction of the metabolic changes is consistent with the opposing cellular actions of insulin receptor and FoxO (5), especially

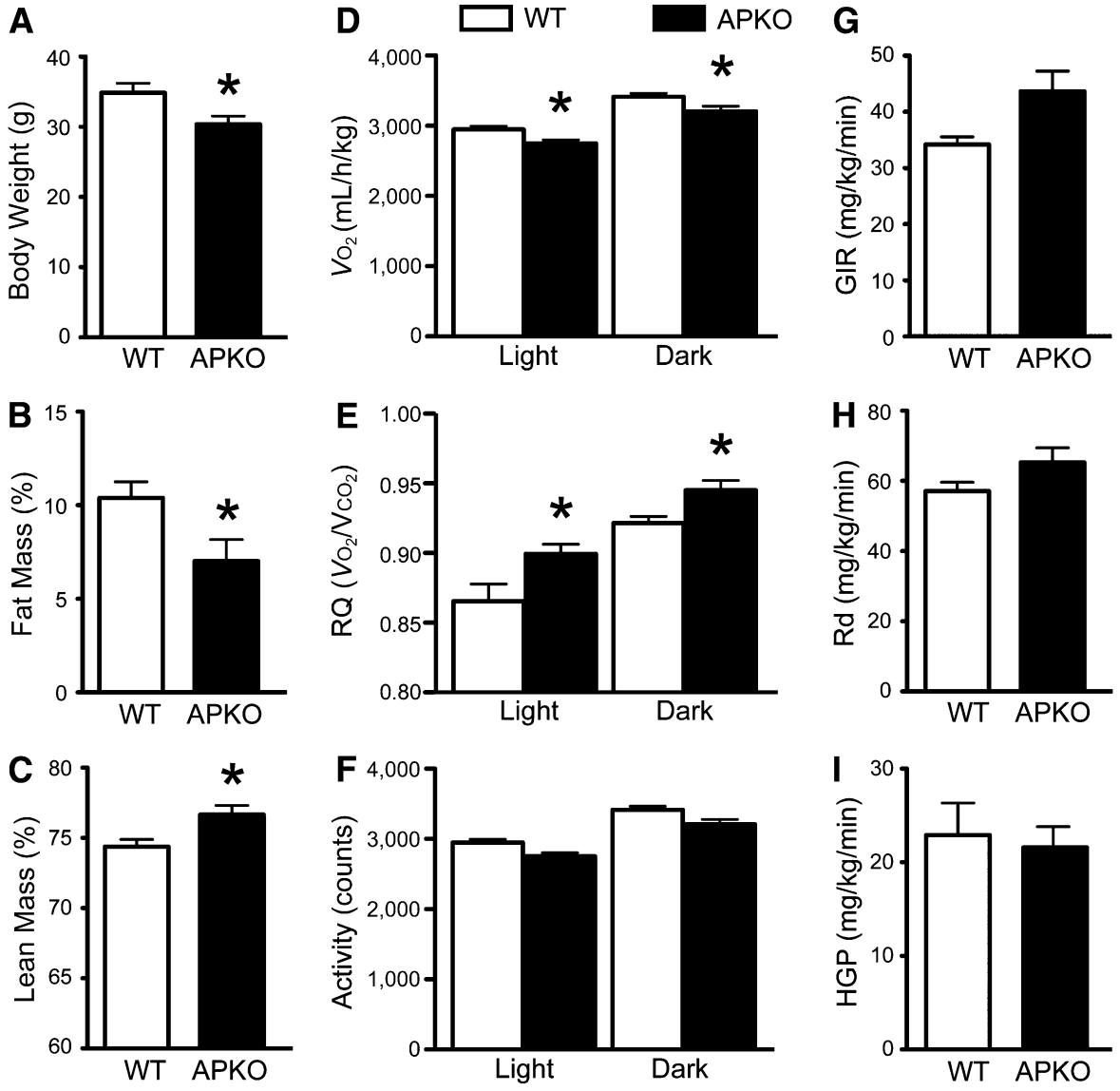

FIG. 7. Distinct energy balance and glucose homeostasis phenotypes of *Pomc;Agrp-Foxo1*$^{-/-}$ mice. Body weight (*A*), fat content (*B*), and lean mass (*C*) (*n* = 8–9 for each genotype). Oxygen consumption (*D*), respiratory quotient (*E*), and locomotor activity (*F*) (*n* = 9 for each genotype). Glucose infusion (*G*), glucose disposal (*H*), and hepatic glucose production (*I*) during euglycemic-hyperinsulinemic clamps (*n* = 4–6 for each genotype). APKO, *Pomc;Agrp-Foxo1*$^{-/-}$; GIR, glucose infusion rate; HGP, hepatic glucose production; Rd, glucose disposal; RQ, respiratory quotient; WT, wild-type. **P* < 0.05.

because the latter acts as a relay node for multiple extracellular signals (32). Similarly, *Syn-Cre* neuron–specific leptin receptor deletion gave rise to obesity associated with increased plasma glucose, insulin, and leptin in a manner that was directly related to the extent of hypothalamic leptin receptor ablation (33). These data lend support to previous work indicating that FoxOs act to integrate insulin with leptin signaling by virtue of their ability to antagonize STAT3 signaling in response to decreasing levels of phospho-Akt (13). Conversely, neuron-specific knockout or knockdown of protein tyrosine phosphatase-1b, a negative regulator of insulin and leptin signaling, improves insulin and leptin sensitivity and protects from diet-induced obesity (34,35). Nonetheless, there are telling differences between the phenotypes resulting from protein tyrosine phosphatase-1b and FoxO ablation, for example, with regard to peripheral metabolism and locomotor activity. These data indicate that FoxO relays multiple pathways acting not only through Akt but also possibly through other kinases. The nature of these kinases and their target sites on FoxO1, as well as the physiologic consequences of their activation on FoxO1 function, represent important areas for further research. In addition to insulin and leptin, FoxO1 mediates the effects of other key hormones on metabolism, such as ghrelin (36). We found in our studies that the diverse, if internally consistent, effects of FoxO ablation on energy homeostasis impinge equally on insulin and leptin signaling, sensitizing the body to both. More challenging is the question of which cellular mechanisms and neuronal relay systems are used to effect these actions.

In this study, we found that mice with FoxO1 knockout in *Syn-Cre*–expressing neurons have increased melanocortin signaling tone, manifested as increased locomotor activity. The finding that constitutively active FoxO1 expression in MBH, but not in SCN, reduces locomotor activity highlights the physiological importance of FoxO1

function in MBH. MBH includes several neuronal populations that are critical for metabolic regulation. For example, FoxO1 activation in POMC and AgRP neurons results in anabolic function, but the underlying effectors and molecular mechanisms are starkly different (12–15,17,18). In POMC neurons, FoxO1 knockout promotes leanness, decreases food intake, increases leptin sensitivity, and increases melanocortin signaling. We have proposed that the key effector of these actions is carboxypeptidase, the protease responsible for cleaving POMC to α-MSH and β-endorphin, which are normally suppressed by FoxO1 (17). In AgRP neurons, FoxO1 regulates expression of AgRP itself (13) and also of the orphan G-protein-coupled receptor Gpr17, whose pharmacological modulation affects food intake and, hence, shows promise as a target of antiobesity drugs (18). Unlike ablation in POMC neurons, ablation in AgRP neurons also had a substantial effect on hepatic glucose production, adding one important potential therapeutic benefit to CNS-targeted FoxO inhibition (18). The ventral medial nucleus is also a site of FoxO1 action (16). Mice lacking FoxO1 in ventral medial nucleus steroidogenic factor-1–expressing neurons are lean because of increased energy expenditure and have increased insulin sensitivity, suggesting that the overarching role of FoxO as a mediator of energy balance extends to multiple CNS sites.

The adult mammalian brain also contains neural stem cells that can give rise to neurons, astrocytes, and oligodendrocytes (37). FoxO1, FoxO3, and FoxO4 cooperatively regulate neural stem cell homeostasis and play important roles in neural stem cell proliferation and renewal, possibly through their regulation of cellular metabolism (27).

FoxO isoforms include FoxO1, FoxO3, and FoxO4. Based on estimates from quantitative PCR analysis, FoxO1 is the major isoform expressed in the brain. FoxO3 is expressed at lower levels, whereas FoxO4 expression is virtually undetectable. These different FoxO isoforms could have functional redundancy, and other isoforms may compensate for the loss of one isoform. For example, this is the case in the liver, where triple ablation of *Foxo* genes causes more pronounced effects than the single FoxO1 knockout with fasting hypoglycemia, increased glucose tolerance and insulin sensitivity, and decreased plasma insulin levels (6). This paradigm appears to hold true in the brain, because our data show that triple FoxO knockouts in the brain are better protected from weight gain induced by HFD, indicating potentially redundant contributions of other FoxO genes to CNS regulation of energy balance.

Understanding the integrative function of FoxO1 in the CNS is crucial for harnessing its therapeutic potential for metabolic diseases. The data presented in this study are reassuring in this regard because we observed no untoward effect of single or triple FoxO ablation. Further, we saw that the effects linked to *Syn-Cre* ablation are qualitatively similar to those observed in more restricted knockouts (16–18), allaying fears that broad-based FoxO inhibition might adversely affect cellular survival, behavior, and overall energy homeostasis.

ACKNOWLEDGMENTS

This study was supported by National Institutes of Health grants DK58282 and DK63608 (Columbia Diabetes Research Center), American Diabetes Association mentor-based fellowship, and Berrie Fellowship Award (H.R.).

No potential conflicts of interest relevant to this article were reported.

H.R. designed and conducted experiments, analyzed data, and wrote the manuscript. L.P.-M. designed and conducted experiments, analyzed data, and wrote the manuscript. R.G.-J. conducted glucose clamp experiments. T.Y.L. and J.Y.K.-M. conducted experiments. G.H. analyzed data. S.L.W. and R.S. designed experiments and analyzed data. D.A. designed experiments, analyzed data, and wrote the manuscript. D.A. is the guarantor of this work and, as such, had full access to all the data in the study and takes responsibility for the integrity of the data and the accuracy of the data analysis.

The authors thank members of the Accili laboratory for insightful data sessions and for critical reading of the manuscript. The authors thank Thomas K. Kolar and Ana M. Flete Castro (Department of Medicine, Columbia University) for excellent technical support. The authors thank Dr. Matthew Butler (Department of Psychology, Columbia University) for helping with wheel-running experiments.

REFERENCES

1. Morton GJ, Schwartz MW. Leptin and the central nervous system control of glucose metabolism. Physiol Rev 2011;91:389–411
2. Gautron L, Elmquist JK. Sixteen years and counting: an update on leptin in energy balance. J Clin Invest 2011;121:2087–2093
3. Suzuki K, Jayasena CN, Bloom SR: Obesity and appetite control. Exp Diabetes Res 2012;2012:824305
4. Varela L, Horvath TL. Leptin and insulin pathways in POMC and AgRP neurons that modulate energy balance and glucose homeostasis. EMBO Rep 2012;13:1079–1086
5. Matsumoto M, Pocai A, Rossetti L, Depinho RA, Accili D. Impaired regulation of hepatic glucose production in mice lacking the forkhead transcription factor Foxo1 in liver. Cell Metab 2007;6:208–216
6. Haeusler RA, Kaestner KH, Accili D. FoxOs function synergistically to promote glucose production. J Biol Chem 2010;285:35245–35248
7. Haeusler RA, Pratt-Hyatt M, Welch CL, Klaassen CD, Accili D. Impaired generation of 12-hydroxylated bile acids links hepatic insulin signaling with dyslipidemia. Cell Metab 2012;15:65–74
8. Talchai C, Xuan S, Lin HV, Sussel L, Accili D. Pancreatic beta cell dedifferentiation as mechanism of beta cell failure in diabetes. Cell 2012;150:1223–1234
9. Nakae J, Kitamura T, Kitamura Y, Biggs WH 3rd, Arden KC, Accili D. The forkhead transcription factor Foxo1 regulates adipocyte differentiation. Dev Cell 2003;4:119–129
10. Kitamura T, Kitamura YI, Funahashi Y, et al. A Foxo/Notch pathway controls myogenic differentiation and fiber type specification. J Clin Invest 2007;117:2477–2485
11. Talchai C, Xuan S, Kitamura T, DePinho RA, Accili D. Generation of functional insulin-producing cells in the gut by Foxo1 ablation. Nat Genet 2012;44:406–412, S1
12. Kim MS, Pak YK, Jang PG, et al. Role of hypothalamic Foxo1 in the regulation of food intake and energy homeostasis. Nat Neurosci 2006;9:901–906
13. Kitamura T, Feng Y, Kitamura YI, et al. Forkhead protein FoxO1 mediates Agrp-dependent effects of leptin on food intake. Nat Med 2006;12:534–540
14. Iskandar K, Cao Y, Hayashi Y, et al. PDK-1/FoxO1 pathway in POMC neurons regulates Pomc expression and food intake. Am J Physiol Endocrinol Metab 2010;298:E787–E798
15. Kim HJ, Kobayashi M, Sasaki T, et al. Overexpression of FoxO1 in the hypothalamus and pancreas causes obesity and glucose intolerance. Endocrinology 2012;153:659–671
16. Kim KW, Donato J Jr, Berglund ED, et al. FOXO1 in the ventromedial hypothalamus regulates energy balance. J Clin Invest 2012;122:2578–2589
17. Plum L, Lin HV, Dutia R, et al. The obesity susceptibility gene Cpe links FoxO1 signaling in hypothalamic pro-opiomelanocortin neurons with regulation of food intake. Nat Med 2009;15:1195–1201
18. Ren H, Orozco IJ, Su Y, et al. FoxO1 target Gpr17 activates AgRP neurons to regulate food intake. Cell 2012;149:1314–1326
19. Paik JH, Kollipara R, Chu G, et al. FoxOs are lineage-restricted redundant tumor suppressors and regulate endothelial cell homeostasis. Cell 2007;128:309–323
20. Butler MP, Karatsoreos IN, LeSauter J, Silver R. Dose-dependent effects of androgens on the circadian timing system and its response to light. Endocrinology 2012;153:2344–2352

21. Lin HV, Plum L, Ono H, et al. Divergent regulation of energy expenditure and hepatic glucose production by insulin receptor in agouti-related protein and POMC neurons. Diabetes 2010;59:337–346
22. Madisen L, Zwingman TA, Sunkin SM, et al. A robust and high-throughput Cre reporting and characterization system for the whole mouse brain. Nat Neurosci 2010;13:133–140
23. Stefater MA, Seeley RJ. Central nervous system nutrient signaling: the regulation of energy balance and the future of dietary therapies. Annu Rev Nutr 2010;30:219–235
24. Thorens B. Sensing of glucose in the brain. Handbook Exp Pharmacol 2012;209:277–294
25. Buteau J, Accili D. Regulation of pancreatic beta-cell function by the forkhead protein FoxO1. Diabetes Obes Metab 2007;9(Suppl. 2):140–146
26. Diano S. New aspects of melanocortin signaling: a role for PRCP in α-MSH degradation. Front Neuroendocrinol 2011;32:70–83
27. Paik JH, Ding Z, Narurkar R, et al. FoxOs cooperatively regulate diverse pathways governing neural stem cell homeostasis. Cell Stem Cell 2009;5:540–553
28. Luiten PG, ter Horst GJ, Buijs RM, Steffens AB. Autonomic innervation of the pancreas in diabetic and non-diabetic rats. A new view on intramural sympathetic structural organization. J Auton Nerv Syst 1986;15:33–44
29. Kreier F, Kap YS, Mettenleiter TC, et al. Tracing from fat tissue, liver, and pancreas: a neuroanatomical framework for the role of the brain in type 2 diabetes. Endocrinology 2006;147:1140–1147
30. Plum L, Belgardt BF, Brüning JC. Central insulin action in energy and glucose homeostasis. J Clin Invest 2006;116:1761–1766
31. Brüning JC, Gautam D, Burks DJ, et al. Role of brain insulin receptor in control of body weight and reproduction. Science 2000;289:2122–2125
32. Eijkelenboom A, Burgering BM. FOXOs: signalling integrators for homeostasis maintenance. Nat Rev Mol Cell Biol 2013;14:83–97
33. Cohen P, Zhao C, Cai X, et al. Selective deletion of leptin receptor in neurons leads to obesity. J Clin Invest 2001;108:1113–1121
34. Bence KK, Delibegovic M, Xue B, et al. Neuronal PTP1B regulates body weight, adiposity and leptin action. Nat Med 2006;12:917–924
35. Picardi PK, Calegari VC, Prada PO, et al. Reduction of hypothalamic protein tyrosine phosphatase improves insulin and leptin resistance in diet-induced obese rats [corrected in Endocriology 2013;154:1667]. Endocrinology 2008;149:3870–3880
36. Varela L, Vázquez MJ, Cordido F, et al. Ghrelin and lipid metabolism: key partners in energy balance. J Mol Endocrinol 2011;46:R43–R63
37. Rafalski VA, Brunet A. Energy metabolism in adult neural stem cell fate. Prog Neurobiol 2011;93:182–203